Bounded Control of an Actuated Lower Limb Orthosis

Hala Rifaï, Walid Hassani, Samer Mohammed and Yacine Amirat

Abstract— **Wearable robots have defined a new horizon for elderly and disabled people, allowing them to regain control of their limbs, as well as for sane people, helping them increase their abilities to execute hard missions. The present paper deals with the control of a lower limb orthosis applied at the knee level. This joint has a great importance in maintaining the human stability in different locomotion phases. A bounded control torque is developed in order to guarantee the asymptotic stability of the knee joint orthosis. The control law respects the physical constraints of the system. Moreover, it is robust with respect to external disturbances. The effectiveness of the control torque is tested in real-time using the EICOSI orthosis of the LISSI Lab.**

I. INTRODUCTION

Nowadays, robots are not only used to execute missions, *e.g.* mobile robots, and afford services, *e.g.* manipulators, but also to assist humans in their living and their daily tasks. This new category of robots is known as wearable robots and work as anthropomorphic devices. Wearable robots are mechatronic systems that fit the geometry of the human body and work in harmony with it. These robots collect signals from the embodying limbs, through some on-board sensors, and transfer adaptable power to the limbs allowing to move them. Defined trajectories of the upper and/or lower limbs can then be executed by applying adequate controls to the anthropomorphic robots' joints. This technique offers to pathologic persons, elderly and people carrying heavy loads the chance to accomplish actions that seemed impossible previously.

Wearable robots are divided into two main categories [1]: exoskeletons and orthoses. The first one is principally used to increase the performance of the wearers in terms of energy economics, joint strength and endurance specially for load transfer purposes. Therefore, they are mainly used in medical and industrial applications [2] as well as military missions [3]. The orthoses refer to mechanisms that assist people suffering of physical weakness in order to help them regain control of their limbs. Their fundamental use covers the domains of rehabilitation and assistance for paralyzed persons and elderly. Although wheel-chairs have solved many problems of displacements, they are not confortable and particularly unadaptable to all environments.

This work lies within the scope of project EICOSI (Exoskeleton Intelligently COmmunicating and Sensitive to Intention), sponsored by the region of Ile-De-France.

H. Rifaï, W. Hassani, S. Mohammed and Y. Amirat are with the Laboratory of Images, Signals and Intelligent Systems (LISSI), EA 3956, University of Paris-Est Créteil, IUT Créteil-Vitry, Dept. R&T, 122 Rue Paul Armangot, 94400 Vitry-Sur-Seine, France. E-mails: {hala.rifai, samer.mohammed, amirat}@u-pec.fr, walid1.hassani@etu.u-pec.fr

Different works have dealt with the control of exoskeletons having multiple degrees of freedom. The control in [3] is based on a scaled compensation of the estimated exoskeleton dynamics and is not sufficiently sensitive to pilot forces. Proportional derivative (PD) feedback is widely used to control the exoskeletons. A PD coupled to a constant-value control, to balance the gravity effect when the foot is on the ground, is applied to control the leg's trajectory and/or stabilize the body at the zero moment point (ZMP) in [4], [5]. A PD with gravity, friction and coriolis forces compensation and a force field controller are developed in [6]. A PD coupled to a disturbance observer is designed in [7]. A fictitious gain is introduced in [8] to balance the changement of body's dynamics during walking, load, etc. and tested with a proportional-integrator-derivative controller (PID). In [9], a proportional control torque is used at the hip level and a control torque proportional to the square of the angular velocity at the knee level while the whole cycle of walking is ensured using a state machine control strategy. Two controllers are developed in [10]: a PD for the inner loop aiming to drive the joints to a desired orientation and a fuzzy logic controller for the outer loop aiming to balance the device at the ZMP. A fuzzy control is also developed in [11] and a neural networks based control in [12] aiming to assist human walking. However, none of these works has proved the exoskeleton's stability.

Exoskeletons or orthoses having only one degree of freedom, at the knee or ankle levels, have also been developed especially for gait rehabilitation. In the sequel, only the works concerning the control of the knee are presented. Some works have proposed to assist people through affording a part of the effort necessary to achieve a movement, allowing to relax their muscles. The desired movement is computed by measuring EMG signals in [13] and the ground reaction force in [14]. The wearer accomplishes a part of the effort while the orthosis ensures the remainder. The controller in this case acts as an amplifier. Note that no desired trajectories are defined and therefore no position controller is used. Another approach consists on modifying the impedance parameters of the human limbs by setting those of the embodied exoskeleton. This strategy allows to increase the leg's natural frequency and facilitates its movement consequently. It is achieved in [15] by modifying the damping parameter with respect to motion intention, used to compute the desired orientation which is tracked by means of PID controller. The exoskeleton and user's inertia compensation is considered in [16] using a positive feedback of low pass-filtered knee's angular acceleration to determine a desired shank orientation. A Linear Quadratic (LQ) controller is designed to reach

the desired orientation. In the last two works, the shank embodying the exoskeleton is modeled as a mass, spring, damper, sparing then all system's non-linearities.
Note that none of the aforecited works has considered the physical constraints of the system. This point is essential in avoiding the saturation of the actuator which may induce instability of the system.

The paper deals with the control of the EICOSI (Exoskeleton Intelligently COmmunicating and Sensitive to Intention) having one degree of freedom at the knee level. In fact, the knee is of great importance in maintaining the stability of the human and ensuring its locomotion specially for elderly and people having impairments at the knee joint level. The orthosis has a simple design, not cumbersome and easy to don and doff which makes it very practical to use by knee-joint disabled persons. The proposed control torque ensures the asymptotic stability of the orthosis. It is bounded in order to take into account the provided power limitation as well as the saturation of the actuator and prevent consequently problems related to nonlinearities. The control law is computed over nested saturation functions of the state feedback, *e.g.* the angular position and velocity, with gravity torque compensation. As a first approach, the wearer is considered completely passive and the totality of the gravity torque is balanced. This is subject to modification in future works namely when introducing the evaluation of human torque, developed by the muscles and measured by EMG electrodes. The control law will balance only the complementary part of the human developed torque, allowing to generate the desired movement.

The paper is structured as follows. The orthosis model as well as its parameters identification are presented in section II. The bounded control torque is proposed in section III and the system's stability is proved. Real-time experimentations are addressed in section IV. Finally, conclusions are presented in section V and future works are introduced.

II. Shank-Orthosis Model and Parameters Identification

The system considered in the present work includes the orthosis as well as the wearer leg. Movements of flexions and extensions of the leg will be studied in a seated position of the wearer.

A. Shank-Orthosis Modeling

As mentioned previously, the design of the orthosis should match the body's geometry. In the project EICOSI, the orthosis is one structure having two segments related along a rotational axis. The first segment embodies the thigh while the second embodies the shank and are fixed to the wearer by means of braces (Fig. 1 and 3). The orthosis and the human leg have, then, the same rotational degree of freedom at the knee level.

Denote by $\mathcal{F}(\vec{x}^f, \vec{y}^f, \vec{z}^f)$ a fixed frame in the space and by $\mathcal{S}(\vec{x}^s, \vec{y}^s, \vec{z}^s)$ a frame attached to the shank at the knee defined such that the direction of $\vec{y}^f$ and $\vec{y}^s$ coincide (Fig. 1).

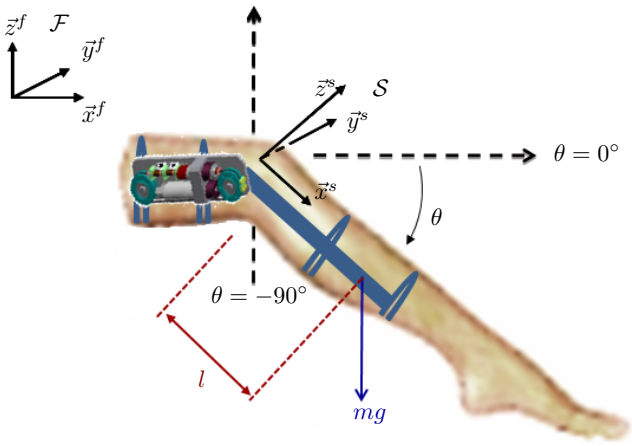

Fig. 1. Human leg embodying the orthosis: Fixed and Shank frames.

The knee, and therefore the orthosis, are in rotation about the pitch axis $\vec{y}^s$ of an angle θ. Since the system has only one degree of freedom, its angular velocity is equal to the derivative of the rotational position. Let θ and $\dot{\theta}$ denote the angular position and velocity of the shank relative to the thigh, respectively. Note that the system (shank and orthosis) behaves as a simple pendulum. In the following, the model of the pendulum movement is given. The shank and orthosis models will be derived similarly. The kinetic and gravitational energies of the simple pendulum are given by:

$$\begin{aligned} E_k &= \frac{1}{2} J\dot{\theta}^2 \\ E_g &= mgl(1-\sin\theta) \end{aligned}$$

with J the inertia of the pendulum system in $\mathcal{S}$, m its mass, l the distance from the knee to the system's center of gravity and g is the gravity acceleration. Deriving the system's Lagrangian $\mathcal{L} = E_k - E_g$, the dynamics of the shank can be written as:

$$J\ddot{\theta} + mgl\cos\theta = \tau_{ext} \tag{1}$$

with τ_{ext} is the external torque acting on the system. It includes the friction torque τ_f and the control torque τ. The solid and viscous frictions are the main components of the friction torque. It is modeled as [17]:

$$\tau_f = -A\text{sign}\dot{\theta} - B\dot{\theta} \tag{2}$$

where A and B are the coefficients of solid and viscous friction torques respectively, sign$(\cdot)$ is the classical sign function. The main advantage of the adopted friction model is the linearity in parameters A and B which facilitates their identification in the sequel.

1) Shank's model: The wearer is considered completely passive. Therefore, he doesn't develop any control torque. The model of the shank can then be written as:

$$J_s\ddot{\theta} + m_s g l_s \cos\theta = -A_s\text{sign}\dot{\theta} - B_s\dot{\theta} \tag{3}$$

with $J_s,\ m_s,\ l_s,\ \ A_s,\ B_s$ are respectively the inertia, mass, distance to the center of gravity, solid and viscous friction coefficients of the shank.

2) Orthosis' model: The orthosis' actuator delivers the whole power to drive the system. Therefore, the model of the orthosis can be written as:

$$J_o\ddot{\theta} + m_o g l_o \cos\theta = -A_o \text{sign}\dot{\theta} - B_o\dot{\theta} + \tau \tag{4}$$

with $J_o,\ m_o,\ l_o,\ \ A_o,\ B_o$ are respectively the inertia, mass, distance to the center of gravity, solid and viscous friction coefficients of the orthosis.

Summing (3) and (4), the system's (orthosis and shank) dynamics can therefore be written as:

$$J\ddot{\theta} = -\tau_g \cos\theta - A\text{sign}\dot{\theta} - B\dot{\theta} + \tau \tag{5}$$

with $J = J_s + J_o$ the system's inertia, $\tau_g = (m_s l_s + m_o l_o)g$ the system's gravity torque in full extension position of the thigh, $A = A_s + A_o$ the system's solid friction coefficient, $B = B_s + B_o$ the system's viscous coefficient and τ the control torque applied by the actuator to drive the orthosis and consequently the shank to a desired orientation.

B. Parameters identification

The shank's and orthosis' parameters are identified separately using the weighted least square method.

1) Shank's parameters: The mass of the shank m_s and the position of its center of gravity l_s are determined based on [18] given the height and weight of the subject. The other parameters are identified using the pendulum test. It consists on dropping the shank from a full extension position till the rest position (see (c) and (a) of Fig. 3). The angle θ is measured using the goniometer SG150 of Biometrics Ltd., attached to the leg at the knee level, such that its local frame coincides with the shank frame $\mathcal{S}$. The angular velocity and acceleration, $\dot{\theta}$ and $\ddot{\theta}$, are derived numerically. (3) can be written as:

$$-m_s g l_s \cos\theta = J_s\ddot{\theta} + A_s\text{sign}\dot{\theta} + B_s\dot{\theta} \tag{6}$$

with J_s, A_s and B_s the parameters to identify.

2) Orthosis' parameters: To identify the orthosis' parameters, an excitation sequence describing the trajectory of the angle θ is predefined as well as the angular velocity and acceleration, $\dot{\theta}$ and $\ddot{\theta}$ [19]. The torque developed by the actuator when subject to the excitation trajectory is computed using measurements of a current sensor. (4) can be rewritten as:

$$\tau = J_o\ddot{\theta} + m_o g l_o \cos\theta + A_o\text{sign}\dot{\theta} + B_o\dot{\theta} \tag{7}$$

with J_o, $m_o g l_o$, A_o and B_o the parameters to identify.

(6) and (7) can be written in the general form:

$$\Gamma_i = W_i(\theta, \dot{\theta}, \ddot{\theta})X + \rho_i \tag{8}$$

where $X \in \mathbb{R}^m$, m is the parameters vector's dimension, Γ_i is the measured/computed torque during identification process, $W_i(\theta, \dot{\theta}, \ddot{\theta})$ is the observation vector and ρ_i is the residue representing measurement noise and modeling error, $i \in \{1, \ldots, n\}$ and n is the number of samples considered within the trajectory and the torques values. Note that $\Gamma = [\Gamma_1 \ldots \Gamma_n]^T \in \mathbb{R}^n$, $W = [W_1 \ldots W_n]^T \in \mathbb{R}^{n\times m}$ and $\rho = [\rho_1 \ldots \rho_n]^T \in \mathbb{R}^n$. The parameters vector $\hat{X} \in \mathbb{R}^m$ is then estimated using the least square optimization:

$$\hat{X} = \text{Arg min } \|\rho\|^2 = W^+\Gamma \tag{9}$$

with $W^+ \in \mathbb{R}^{m\times n}$ the pseudo-inverse of matrix W given by $W^+ = (W^TW)^{-1}W^T$. Note that ρ is considered as a vector of white noise having a null mean vector.

III. Exoskeleton Control

Controlling the knee joint is of great importance in maintaining the equilibrium of a person in standing-up position as well as in facilitating the locomotion during swinging-phase. Therefore, a robust control should be applied to the orthosis in order to ensure the stability of the person embodying it. This control law should take into consideration two criteria related principally to the safety of the mechanism since it is in direct relation with the human body. Quick variations of the friction, induced by unpredictable movements and causing wear loading of the actuator, engender unacceptable behavior of the orthosis. Therefore, it is not preferable to balance the friction in the control law in order to avoid quick changes in its value. On the other hand, a high value of the control torque necessitates high power to ensure it, which can not be achieved in wearable robots because it affects the safety of the wearer. Besides, the saturation of the actuators can lead to undesirable closed loop behaviors resulting in robot's instability. Consequently, the actuator amplitude limitation should be taken into consideration in the design of the control torque in order to avoid irreversible damages and maximize its effectiveness.

Bounded control has been treated in the literature for systems falling in the framework of integrators chains [20], [21], [22], [23], [24], rigid bodies [25] and manipulators [26], [27], [28]. Note that the last case of applications is of interest in the present work because the orthosis falls within the framework of manipulators. For these applications, the gravity balance should be taken into consideration. The aforecited control laws of manipulators are mainly based on saturated PD/PID or composed of the sum of the saturations applied individually to proportional and derivative terms. In the present work, a control torque based on nested saturations is proposed allowing not only to maintain bounded inputs, but also to have a better management of the velocity and position convergence. This control law takes into account the system's physical constraints. It is low cost in terms of computations, therefore it is adapted for real-time applications like the orthosis, subject of interest of the present paper. Moreover, it ensures the asymptotic stability of the system.

Before establishing the control torque, some definition and properties are given.

Definition 1: A saturation function $\text{sat}_N(x)$, bounded between $\pm N$, is defined such as:

$$\text{sat}_N(x) = \begin{cases} x & \text{if} \quad |x| \le N \\ N\text{sign}(x) & \text{if} \quad |x| > N \end{cases} \tag{10}$$

with $x \in \mathbb{R}^+$ and sign$(\cdot)$ the classical sign function.

Properties 1: The saturation function verifies the following properties:

1) $x\,\text{sat}_N(x) > 0\ \forall x \neq 0$
2) $\text{sat}_N(x) = 0$ if and only if $x = 0$
3) $|\text{sat}_N(x)| \leq N$

The control torque and stability analysis are presented in the following:

Proposition 1: Consider the knee-joint human-orthosis model described by (5) with θ and $\dot{\theta}$ the knee joint angle and angular velocity, respectively. Denote θ_d the desired orientation and $\tilde{\theta} = \theta - \theta_d$ the orientation error. The control torque bounded between $\pm\bar{\tau}$ and defined by:

$$\tau = -\text{sat}_{N_1}[k_1\dot{\theta} + \text{sat}_{N_2}(k_2\tilde{\theta})] + \tau_g \cos\theta \tag{11}$$

asymptotically stabilizes (5) at $(\theta, \dot{\theta}) = (\theta_d, 0)$ with a domain of attraction equal to $[-\theta_{max}, 0] \times \mathbb{R}$. k_1 and k_2 are positive scalar parameters and $\text{sat}_{N_i}(\cdot)$, $i \in \{1, 2\}$, are saturation functions defined in (10) with N_i the saturation bounds chosen such that $N_1 > 2N_2 > 2A$. The saturation bound of the control torque is $\bar{\tau} = N_1 + \tau_g$.

Proof: Consider firstly that $k_2|\tilde{\theta}| > N_2$ and $k_1|\dot{\theta}| > N_1 - N_2 > N_2$.
Consider the Lyapunov function V positive definite and radially unbounded:

$$V = \frac{1}{2}J\dot{\theta}^2 \tag{12}$$

Based on the system's model (5) and the control torque (11), the derivative of the Lyapunov function V is given by:

$$\begin{aligned}\dot{V} &= \dot{\theta}\big(-\tau_g\cos\theta - B\dot{\theta} - A\text{sign}\dot{\theta} + \tau_g\cos\theta \\ &\qquad -\text{sat}_{N_1}[k_1\dot{\theta} + \text{sat}_{N_2}(k_2\tilde{\theta})]\big) \\ &= -B\dot{\theta}^2 - A\dot{\theta}\text{sign}\dot{\theta} - \dot{\theta}\text{sat}_{N_1}[k_1\dot{\theta} + \text{sat}_{N_2}(k_2\tilde{\theta})]\end{aligned}$$

Since $|k_1\dot{\theta}| > N_2$, then $|k_1\dot{\theta} + \text{sat}_{N_2}(k_2\tilde{\theta})| > 0$. Therefore, $\dot{\theta}$ and $k_1\dot{\theta} + \text{sat}_{N_2}(k_2\tilde{\theta})$ are of the same sign. The Lyapunov function becomes:

$$\dot{V} = -B\dot{\theta}^2 - A\dot{\theta}\text{sign}\dot{\theta} - |\dot{\theta}|N_1 \tag{13}$$

The Lyapunov function V is decreasing and $|\dot{\theta}|$ consequently. $\dot{\theta}$ enters the set $\Omega_1 : \{\dot{\theta}, \tilde{\theta} : k_1|\dot{\theta}| < N_1 - N_2, k_2|\tilde{\theta}| > N_2\}$. In Ω_1, $k_1|\dot{\theta}| + N_2 < N_1$. $\text{sat}_{N_1}(\cdot)$ operates then in the linear region and the control torque (11) becomes:

$$\tau = -k_1\dot{\theta} - \text{sat}_{N_2}(k_2\tilde{\theta}) + \tau_g\cos\theta \tag{14}$$

In Ω_1, define the Lyapunov function W as:

$$W = \frac{1}{2}J(\dot{\theta}+\lambda\tilde{\theta})^2 + \tilde{\theta}\text{sat}_{N_2}(k_2\tilde{\theta}) + \frac{1}{2}\lambda(B+k_1-J\lambda)\tilde{\theta}^2 \tag{15}$$

with $0 < \lambda < \frac{B+k_1}{J}$ and $\kappa = N_2 - A > 0$.
The derivative of the Lyapunov function within the trajectories of the system is given by:

$$\begin{aligned}\dot{W} &= (\dot{\theta}+\lambda\tilde{\theta})(J\ddot{\theta} + J\lambda\dot{\theta}) + \dot{\theta}\text{sat}_{N_2}(k_2\tilde{\theta}) \\ &\qquad +\tilde{\theta}\frac{d}{dt}(\text{sat}_{N_2}(k_2\tilde{\theta})) + \lambda(B+k_1-J\lambda)\tilde{\theta}\dot{\theta} \\ &= (\dot{\theta}+\lambda\tilde{\theta})[-(B+k_1-J\lambda)\dot{\theta} - A\text{sign}\dot{\theta} \\ &\qquad -\text{sat}_{N_2}(k_2\tilde{\theta})] + \dot{\theta}\text{sat}_{N_2}(k_2\tilde{\theta}) \\ &\qquad +\tilde{\theta}\dot{\theta}\frac{d}{d\tilde{\theta}}(\text{sat}_{N_2}(k_2\tilde{\theta})) + \lambda(B+k_1-J\lambda)\tilde{\theta}\dot{\theta}\end{aligned}$$

Since $k_2|\tilde{\theta}| > N_2$ then $|\text{sat}_{N_2}(k_2\tilde{\theta})| = N_2$ and $\frac{d}{d\tilde{\theta}}(\text{sat}_{N_2}(k_2\tilde{\theta})) = 0$. The derivative of the Lyapunov function W becomes:

$$\begin{aligned}\dot{W} &= -(B+k_1-J\lambda)\dot{\theta}^2 - A\dot{\theta}\text{sign}\dot{\theta} - \lambda\tilde{\theta}\text{sat}_{N_2}(k_2\tilde{\theta}) \\ &\qquad -A\lambda\tilde{\theta}\text{sign}\dot{\theta} \\ &\leq -(B+k_1-J\lambda)\dot{\theta}^2 - A\dot{\theta}\text{sign}\dot{\theta} - \lambda|\tilde{\theta}|N_2 + A\lambda|\tilde{\theta}| \\ &\leq -(B+k_1-J\lambda)\dot{\theta}^2 - A\dot{\theta}\text{sign}\dot{\theta} - \lambda|\tilde{\theta}|\kappa\end{aligned}$$

W is then decreasing. $\dot{\theta}$, $\tilde{\theta}$ enter the set Ω_2 defined by $\Omega_2 : \{\dot{\theta}, \tilde{\theta} : k_1|\dot{\theta}| < N_1 - N_2, k_1|\tilde{\theta}| < N_2\}$. In Ω_2, $\text{sat}_{N_2}(\cdot)$ operates in the linear region and the control torque (14) becomes:

$$\tau = -k_1\dot{\theta} - k_2\tilde{\theta} + \tau_g\cos\theta \tag{16}$$

Define in Ω_2 the Lyapunov function L as:

$$L = \frac{1}{2}J\dot{\theta}^2 + \frac{1}{2}k_2\tilde{\theta}^2 \tag{17}$$

Replacing (16) in (5), the derivative of the Lyapunov function L is given by:

$$\dot{L} = -(B+k_1)\dot{\theta}^2 - A\dot{\theta}\text{sign}\dot{\theta} \leq 0 \tag{18}$$

The Lyapunov function L is then decreasing till the angular velocity reaches the origin $\dot{\theta} \equiv 0$. In order to complete the proof, the LaSalle Invariance Principle is invoked. All the trajectories converge to the largest invariant set $\bar{\Omega}_3$ in $\Omega_3 = \{(\tilde{\theta}, \dot{\theta}) : \dot{L} = 0\} = \{(\tilde{\theta}, \dot{\theta}) : \dot{\theta} = 0\}$. To remain in this set, one must ensure that $J\ddot{\theta} = -k_2\tilde{\theta} = 0$ with $k_2 > 0$. Therefore, to remain in the set $\bar{\Omega}_3$, one should satisfy $\tilde{\theta} = 0$ which means that $\theta = \theta_d$. Therefore, $(\theta, \dot{\theta}) = (\theta_d, 0)$ is an asymptotically stable point of the closed-loop system with domain of attraction equal to $[-\theta_{max}, 0] \times \mathbb{R}$. ■

IV. Experimentation and Robustness tests

The control law is tested in real-time using the EICOSI orthosis of the Laboratory of Images, Signals and Intelligent Systems (LISSI) of the University of Paris-Est Créteil (UPEC). The mechanical structure of the orthosis consists of two segments attached to the thigh and shank respectively by means of braces, with a rotation axis at the knee level. The orthosis is actuated using a brushless DC motor (BLDC) chosen because it delivers a relatively high torque and runs smoothly at low speeds. The maximal torque that can be delivered by the actuator is $\bar{\tau} = 13\,N \cdot m$. The orthosis is also equipped with an incremental encoder that delivers

the angle of the shank segment relative to the thigh one. The control torque is computed using a controller board (dSPACE-DS1103) equipped with an IBM processor (PowerPC 604th) running at $400\,Mhz$. The controller takes the measurement of the angle delivered by the EICOSI's sensor and the angular velocity obtained by a simple derivation as well as the desired angle and velocity. The controller board delivers the pulse width modulation (PWM) level to control the actuator's velocity. The control loop runs at $1\,kHz$, fixed due to current and position sensors constraints.
The bloc diagram is presented in Fig. 2.

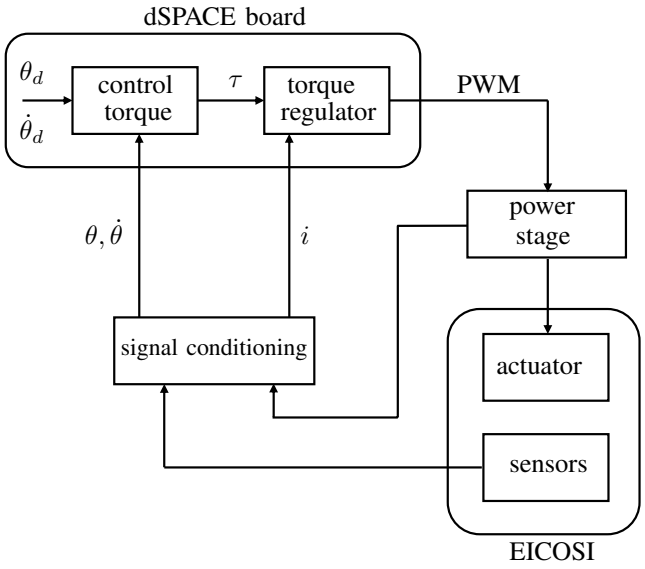

Fig. 2. Bloc diagram of the actuated orthosis in closed loop

The experiments are conducted on a sane subject having 27 years old, weighing $90\,Kg$ and measuring $1.87\,m$.

The parameters identification of the subject and the orthosis are described in section II. The desired trajectory of the shank, considered during identification phase, is given by:

$$q(t) = \sum_{i=1}^{n} \frac{a_l}{\omega_f l} \sin(\omega_f l t) - \frac{b_l}{\omega_f l} \cos(\omega_f l t) + q_0 \qquad (19)$$

with ω_f is the fundamental radian frequency of the Fourier series, $\frac{a_l}{\omega_f l}$ and $\frac{b_l}{\omega_f l}$ are the amplitudes of the sine and cosine functions, t is the time and q_0 is the initial value of the trajectory. The optimization is performed using the following conditions:

$$\begin{array}{rcccl} -\frac{\pi}{2}\,rad & \leq & \theta & \leq & 0\,rad \\ -2.1\,rad/s & \leq & \dot{\theta} & \leq & 2.1\,rad/s \\ -\pi\,rad/s^2 & \leq & \ddot{\theta} & \leq & \pi\,rad/s^2 \end{array} \qquad (20)$$

The system's (shank and orthosis) identified parameters: inertia J, solid and viscous coefficients A and B, the gravity torque τ_g are given in TABLE I.

The saturation bounds of the control torque defined in (11) are set such that it respects the limitation of the supplied power and the maximal torque delivered by the actuator. Therefore, $N_1 = 8$ and $N_2 = \frac{8}{2.1}$. The control parameters are set to: $k_1 = 20$ and $k_2 = 75$.

Parameter	Symbol	Value
Inertia	J	$0.4\,Kg \cdot m^2$
Solid friction coefficient	A	$0.6\,N \cdot m$
Viscous friction coefficient	B	$1\,N \cdot m \cdot s \cdot rad^{-1}$
Gravity torque	τ_g	$5\,N \cdot m$

TABLE I
SYSTEMS PARAMETERS IDENTIFICATION

Two experiments are performed to test the efficiency of the control law.

The first considers flexions and extensions of the knee,

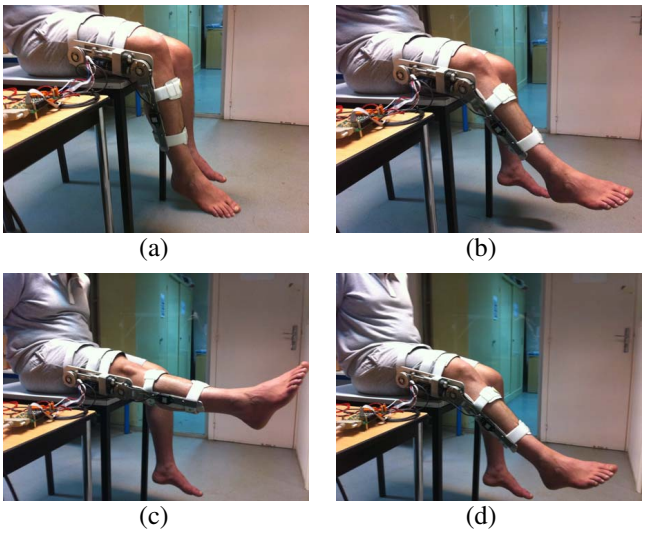

Fig. 3. Successive positions of the shank during flexion-extension: (a) shows the rest position, (b) presents the shank during extension, (c) shows the full extension position and (d) the shank during flexion phase.

actions that are often achieved in rehabilitation phases. The desired trajectory is considered as successive steps. The control torque (11) is applied. (Fig. 3) shows snapshots of the system's (shank + orthosis) trajectory. The angle, angular velocity and control torque are plotted in Fig. 4. Experiments show a good convergence of the angle at adaptable time. The control torque remains within the saturation bounds avoiding the nonlinearities of the actuator. The angular velocity is not high, avoiding the wearer to endure high velocities that may be harmful for disabled people. When the shank reaches the desired position, the angular velocity is null and the control torque balances the shank and orthosis' weight. If the desired position is the full extension defined by angle $\theta = 0\,deg$, the control torque will the value of τ_g. The second experiment considers a path tracking during locomotion phase of a person. A sinusoidal reference trajectory is considered. Control torque (11) is applied on the dynamics errors. The angle, angular velocity and control torque are presented in Fig. 5. The experiments show a good tracking of the angle and angular velocity, besides acceptable values of angular velocity and torque, which guarantees the safety of the wearer.

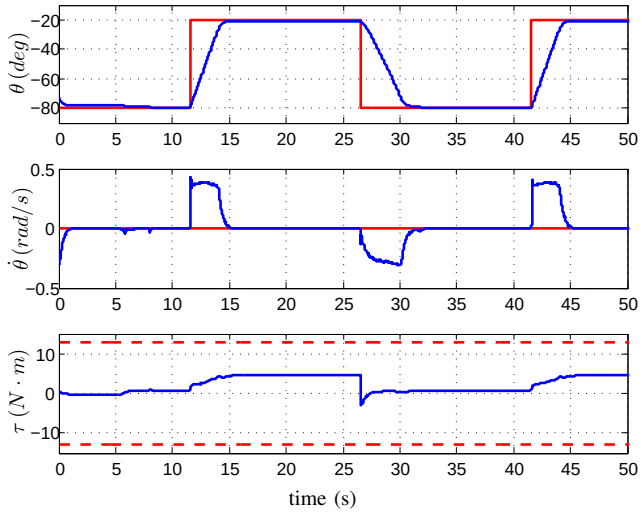

Fig. 4. Flexions and extensions: The knee-joint angle, angular velocity and control torque. The current values are plotted in blue, the desired values in continuous red lines, and the torque saturation bound in dashed red line.

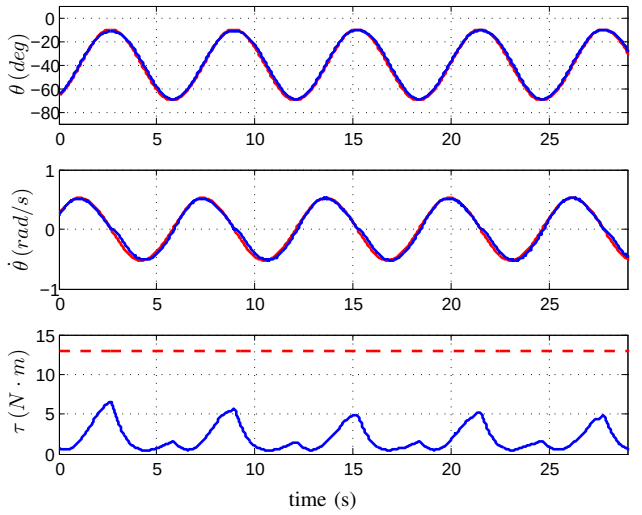

Fig. 5. Sinusoidal trajectory: The knee-joint angle, angular velocity and control torque. The current values are plotted in blue, the desired values in continuous red lines, and the torque saturation bound in dashed red line.

A. Robustness with respect to parameters identification

The control law is independent of the system's inertia, solid and viscous friction coefficients. However, the saturation bound of the scaled orientation error should always satisfy $N_2 > A$ to guarantee stability. The control depends only of the gravity torque. A bad estimation of this parameter does not induce instability. It would only create a static error, *i.e.* the shank does not follow exactly the desired trajectory including flexion and extension. Note that, during tests, τ_g can be adjusted in the control law to fit perfectly the wearer. This can be achieved technically using a simple potentiometer.

B. Robustness with respect to external disturbances

A wrong movement at the knee level can cause instability or even giving way. Therefore, one main property of the control law is to regain the intended position whenever an unpredictable flexion occur. In other words, the control law should be robust to external disturbances that may affect the knee and consequently the whole stability and safety of the wearer. Some experiments showing the robustness of the control law are presented in Fig. 6 and 7 in both cases : flexion/extension and sinusoidal trajectory, respectively. In the first case, the control torque reaches the saturation bound before regaining stability. The saturation helps limiting the current used by the actuator to develop the desired torque and avoids its saturation consequently. In the second case, the disturbance effect is almost not noticeable on the system's trajectory. In both cases, the angular velocities remain acceptable for the user.

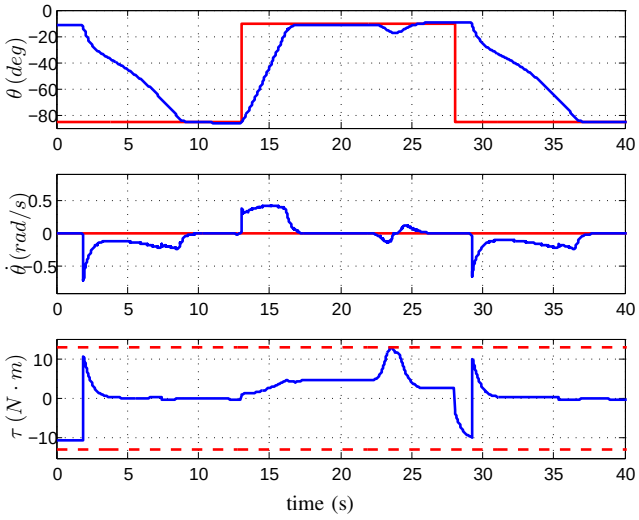

Fig. 6. Flexions and extensions in presence of external disturbances: The knee-joint angle, angular velocity and control torque. The current values are plotted in blue, the desired values in continuous red lines, and the torque saturation bound in dashed red line.

V. Conclusions and Future Works

The present paper treated the control of a knee-joint orthosis. For this purpose, a model, of the shank and orthosis, has been proposed and its parameters has been identified using the weighted least-square method. A bounded control torque based on nested saturations with a gravity compensation has been proposed and its asymptotic stability has been proved using Lyapunov analysis. The control is low cost in terms of computation, independent of the system's inertia and friction model. Moreover, it is robust with respect to external disturbances allowing to guarantee the stability of the wearer in case of a wrong movement at the knee level. The proposed control has been tested in real-time using the EICOSI orthosis of the LISSI Lab. Note that the present work considers a completely passive wearer. Future works will integrate the contribution of the wearer by means of its muscle's effort. This effort will be measured using EMG

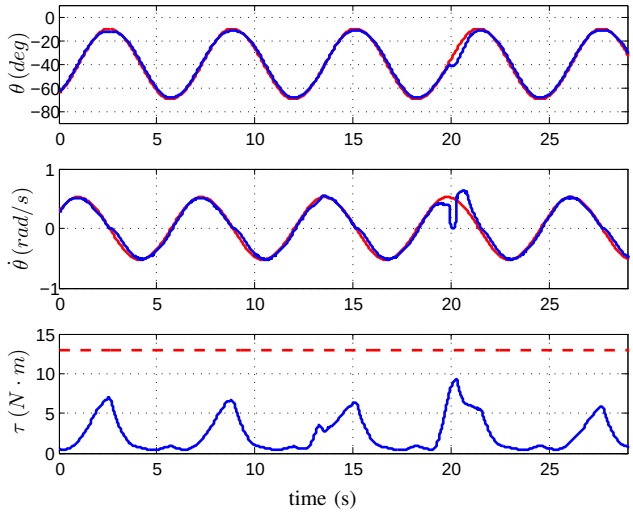

Fig. 7. Sinusoidal trajectory in presence of external disturbances: The knee-joint angle, angular velocity and control torque. The current values are plotted in blue, the desired values in continuous red lines, and the torque saturation bound in dashed red line.

signals. The development of an exoskeleton to control more degrees of freedom of the lower limbs is also envisaged.

REFERENCES

[1] H. Herr, "Exoskeletons and orthoses: classification, design challenges and future directions," *Journal of NeuroEngineering and Rehabilitation*, vol. 6, no. 21, 2009.

[2] H. Satoh, T. Kawabata, and Y. Sankai, "Bathing care assistance with robot suit HAL," in *Proceedings of International Conference on Robotics and Biomimetics*, China, 2009, pp. 498–503.

[3] H. Kazerooni, J.-L. Racine, L. Huang, and R. Steger, "On the control of the Berkeley lower extremity exeskeleton (BLEEX)," in *Porceedings of the International Conference on Robotics and Automation*, Barcelona, Spain, 2005, pp. 4364–4371.

[4] K. Suzuki, G. Mito, H. Kawamoto, Y. Hasegawa, and Y. Sankai, "Intention-based walking support for paraplegia patients with robot suit HAL," *Journal of Advanced Robotics*, vol. 21, no. 1, pp. 1441–1469, 2007.

[5] A. Tsukahara, R. Kawanishi, Y. Hasegawa, and Y. Sankai, "Sit-to-stand and stand-to-sit transfer support for complete paraplegic patients with robot suit HAL," *Journal of Advanced Robotics*, vol. 24, no. 1, pp. 1615–1638, 2010.

[6] S.-K. Banala, A. Kulpe, and S.-K. Agrawal, "A powered leg orthosis for gait rehabilitation of motor-impaired patients," in *Porceedings of the International Conference on Robotics and Automation*, Roma, Italy, 2007, pp. 4140–4145.

[7] K. Kong, H. Moon, B. Hwang, D. Jeon, and M. Tomizuka, "Impedance compensation of SUBAR for back-drivable force-mode actuation," *IEEE Transactions on Robotics*, vol. 25, no. 3, pp. 512–521, 2009.

[8] K. Kong and M. Tomizuka, "Control of exoskeletons inpeired by fictitious gain in human model," *IEEE/ASME Transactions on Mechatronics*, vol. 14, no. 6, pp. 689–698, 2009.

[9] C.-J. Walsh, K.-P. Pasch, and H. Herr, "An autonomous, underactuated exoskeleton for load carrying augmentation," in *Proceedings of International Conference on Intelligent Robots and Systems*, Beijing, China, 2006, pp. 1410–1415.

[10] N. Aphiratsakun and M. Parnichkun, "Balancing control of AIT Leg Exoskeleton using ZMP based FLC," *International Journal of Advanced Robotics Systems*, vol. 6, no. 4, pp. 319–328, 2009.

[11] K. Kong and D. Jeon, "Design and control of an exeskeleton for the elderly and patients," *IEEE/ASME Transactions on Mechatronics*, vol. 11, no. 4, pp. 428–432, 2006.

[12] C.-J. Yang, B. Niu, and Y. Chen, "Adaptive neuro-fuzzy control based development of a wearable exoskeleton leg fo human walking power augmentation," in *Proceedings of International Conference on Advanced Intelligent Mechatronics*, CA, USA, 2005, pp. 467–472.

[13] C. Fleischer and G. Hommel, "A human-exeskeleton interface utilizing electromyography," *IEEE Transactions on Robotics*, vol. 24, no. 4, pp. 872–882, 2008.

[14] J.-E. Pratt, B.-T. Krupp, C.-J. Morse, and S.-H. Collins, "The RoboKnee: An exoskeleton for enhancing strength and endurance during walking," in *Porceedings of the International Conference on Robotics and Automation*, New Orleans, USA, 2004, pp. 2430–2435.

[15] G. Aguirre-Ollinger, J.-E. Colgate, M.-A. Peshkin, and A. Groswami, "A 1-DOF assistive exoskeleton with virtual negative damping: Effects on the kinematic response of the lower limbs," in *Proceedings of International Conference on Intelligent Robots and Systems*, San Diego, CA, USA, 2007, pp. 1938–1944.

[16] ——, "Design of an active 1-DOF lower-limb exoskeleton with inertia compensation," *International Journal of Robotics Research*, 2010.

[17] W.-B. Dunbar, R.-A. de Callafon, and J.-B. Kosmatka, "Coulomb and viscous friction fault detection with application to a pneumatic actuator," in *Proceedings of IEEE/ASME International Conference on Advanced Intelligent Mechatronics*, vol. 2, Como, Italy, 2001, pp. 1239–1244.

[18] D.-A. Winter, *Biomechanics and motor control of human movement*, 4^{th} ed., Wiley, Ed. John Wiley & Sons, 2009.

[19] J. Swevers, C. Ganseman, D. Bilgin, J. De Schutter, and H. Van Brussel, "Optimal robot excitation and identification," *IEEE Transactions on Robotics and Automation*, vol. 13, no. 5, pp. 730–740, 1997.

[20] A. Teel, "Global stabilization and restricted tracking for multiple integrators with bounded controls," *Systems & Control Letters*, vol. 18, no. 3, pp. 165–171, 1992.

[21] H. Sussmann, E. Sontag, and Y. Yang, "A general result on the stabilization of linear systems using bounded controls," *IEEE Transactions on Automatic Control*, vol. 39, no. 12, pp. 2411–2425, 1994.

[22] E. N. Johnson and S. K. Kannan, "Nested saturation with guaranteed real poles," in *American Control Conference*, vol. 1, 2003, pp. 497–502.

[23] N. Marchand and A. Hably, "Global stabilization of multiple integrators with bounded controls," *Automatica*, vol. 41, no. 12, pp. 2147–2152, 2005.

[24] N. Marchand, "Further results on global stabilization for multiple integrators with bounded controls," in *IEEE Conference on Decision and Control, CDC'2003*, vol. 5, Hawai, USA, 2003, pp. 4440–4444.

[25] J. Guerrero-Castellanos, A. Hably, N. Marchand, and S. Lesecq, "Bounded attitude stabilization: Application on four rotor helicopter," in *Proceedings of the 2007 IEEE Int. Conf. on Robotics and Automation*, Roma, Italy, 2007, pp. 730–735.

[26] J. Alvarez-Ramirez, R. Kelly, and I. Cervantes, "Semiglobal stability of saturated linear PID control for robot manipulators," *Automatica*, vol. 39, no. 6, pp. 989–995, 2003.

[27] A. Zavala-Rio and V. Santibañez, "A natural staurating extension of the PD-with-desired-gravity-compensation control law for robot manipulators with bounded inputs," *IEEE Transactions on Robotics*, vol. 23, no. 2, pp. 386–391, 2007.

[28] E. Aguiñaga-Ruiz, A. Zavala-Rio, V. Santibañez, and F. Reyes, "Global trajectory tracking through static feedback for robot manipulators with bounded inputs," *IEEE Transactions on Control Systems Technology*, vol. 17, no. 4, pp. 934–944, 2009.